USING PAVEMENT MARKINGS TO SUPPORT THE QA/QC OF LIDAR DATA

C. Toth [a, *], E. Paska[a], D. Brzezinska [b]

[a] Center for Mapping, OSU, 1216 Kinnear Road, Columbus, OH 43212 USA - (toth, eva-paska)@cfm.ohio-state.edu
[b] Dept. of Civil and Environmental Engineering and Geodetic Science, OSU, dbrzezinska@osu.edu

Commission I, WG I/2

KEY WORDS: LiDAR, LiDAR intensity, Feature extraction, QA/QC

ABSTRACT:

LiDAR technology became an indispensable airborne mapping tool in recent years and is the primary source of highly accurate surface data at large scale. Although, the ranging accuracy of the laser sensor strongly depends on the surface characteristics, by and large, it falls in to the few cm range. This also implies that the achieved accuracy of a LiDAR system, defined in terms of the absolute accuracy of the laser points, is predominantly determined by the quality of the navigation solution (typically based on GPS/IMU sensor integration). Despite significant advancements in navigation technologies recently, to achieve and sustain a high accuracy navigation solution of an airborne platform for extended time is still a difficult task. Furthermore, there is no reliable way to assess the positioning quality of the data captured by any imaging sensor systems, which are based on direct georeferencing. Therefore, using some ground control is almost mandatory if high accuracy is required. This paper introduces a method to use road pavement marking as ground control that could be used for QA/QC. These linear features are widely available in urban areas and along transportation corridors, where most of the government and commercial mapping takes place. A key advantage of using pavement markings is that they can be quickly surveyed with GPS VRS technique.

1. INTRODUCTION

The introduction of airborne LiDAR (Light Detection And Ranging) in the late nineties was followed by a quick proliferation of the technology, and LiDAR is now the primary surface data extraction mapping technique. This remarkable success is mainly due to the fact that LiDAR data are explicit and the processing can be highly automated plus that an unprecedented vertical accuracy could be obtained relatively easily. The horizontal accuracy of the LiDAR data was not a concern in the early use of this technology. In fact, the first LiDAR data QA/QC and product characterization effort did only deal with the vertical accuracy (ASPRS, 2004).

As the LiDAR market started to grow rapidly, soon the LiDAR systems showed truly phenomenal performance improvements. In less than five years, the pulse rate improved by an order and now 100 and 150 kHz systems are widely used (Optech, 2006 and Leica, 2006) and experimental two-pulse systems are also available. More importantly, the ranging accuracy has increased substantially and now stands close to the level of static GPS surveys, i.e., 1-2 cm for hard surfaces, which is practically negligible to the typical navigation error budget. This remarkable performance potential of the newer LiDAR systems, combined with better operational techniques, opened the door toward applications where large-scale or engineering-scale accuracy is required. At this point the georeferencing error budget and, to a lesser extent, the sensor calibration quality, are critical to achieving engineering design level accuracy (few cm). Using ground control is an effective way to compensate for georeferencing and sensor modeling errors. In addition, ground control can provide for independent and highly reliable QA/QC processes.

This paper proposes a method to use road pavement markings as ground control to assess the quality of the LiDAR data as well as to improve the point cloud accuracy by post-processing. Beyond their wide availability, the use of pavement markings is primarily motivated by the fact that they can be rather easily surveyed using GPS VRS (Virtual Reference System) technology; the process is fast, typically it takes one minute to survey a point, and the accuracy, in general, is about 2-3 and 3-6 cm horizontally and vertically, respectively.

2. LIDAR ACCURACY AND ERROR CORRECTION TECHNIQUES

The errors in laser scanning data can come from individual sensor calibration or measurement errors, lack of synchronization, or misalignment between the different sensors. Baltsavias (1999) presents an overview of the basic relations and error formulae concerning airborne laser scanning. Schenk (2001) provides a summary of the major error sources for airborne laser scanners and error formulas focusing on the effect of systematic errors on point positioning. In general, LiDAR sensor calibration includes scan angle, range calibration and intensity-based range correction. The LiDAR sensor platform orientation is always provided by a GPS/IMU-based integrated navigation system. The connection between the navigation and LiDAR sensor frames is described by the mounting bias, which is composed of the offset between the origin of the two coordinate systems and the boresight misalignment (the boresight misalignment describes the rotation between the two coordinate systems, and is usually expressed by roll, pitch and heading angles). To achieve optimal error compensation that assures the highest accuracy of the final product, all of these parameters should be calibrated. Since not all of the parameters can be calibrated in a laboratory

* Corresponding author.

environment, a combination of laboratory and in situ calibrations is the only viable option for LiDAR system calibration. Typical anomalies in the LiDAR data indicating system calibration errors are: edges of the strips could bend up or down (scan angle error), horizontal surfaces have a visible mismatch between the known and the LiDAR point-defined surfaces (boresight misalignment or navigation error), vertical coordinates of LiDAR points over flat areas do not match the known vertical coordinate of the area (ranging or navigation error), objects, such as pavement markings made of retro reflective coatings, may show up above the surface level, although they should practically have identical vertical coordinates (lack of intensity correction of the range data), etc.

The techniques to detect and ultimately compensate for errors fall into two broad categories based on whether they use absolute control or not. The first group includes most of the strip adjustment techniques and some of the sensor and boresight calibration methods. The ground control-based techniques encompass comparisons to reference surfaces, such as parking lots and buildings, and methods using LiDAR-specific control targets.

Strip adjustment methods primarily minimize the vertical discrepancies between overlapping strips or between strips and horizontal control surfaces. These strip adjustments can be referred to as one-dimensional strip adjustment methods (Crombaghs et al., 2000; Kager and Kraus, 2001); tie or absolute control features used for this adjustment are flat horizontal surfaces. The problem with this kind of adjustment is that existing planimetric errors are likely to remain in the data. Vosselman and Maas (2001) have shown that systematic planimetric errors are often much more significant than vertical errors in LiDAR data and, therefore, a 3D strip adjustment is the desirable solution minimizing the 3D discrepancies between overlapping strips and at control points. A number of 3D adjustment methods have been published. Kilian et al. (1996) presented a method of transforming overlapping LiDAR strips to make them coincide with each other using control and tie points in a way similar to photogrammetric block adjustment. Burman (2002) treated the discrepancies between overlapping strips as positioning and orientation errors with special attention given to the alignment error between the IMU and laser scanner (Soininen, 2005). Filin (2003) presented a similar method for recovering the systematic errors; the method is based on constraining the position of the laser points to the surface from which it was reflected. Toth et al. (2002) presented a method that tried to make overlapping strips coincide, with the primary objective of recovering the boresight misalignment between the IMU and laser sensor.

LiDAR-specific ground control targets were introduced by Toth and Brzezinska (2005; Csanyi et al., 2005). The proposed technique uses ground control targets specifically designed for LiDAR data to provide quality control for applications that require cm-level, engineering scale mapping accuracy. Simulation results confirmed that the optimal target is rotation invariant, circular-shaped, elevated from the ground and that a flat target with 1 m circle radius can provide sufficient accuracy from a point density of about 5 pts/m2. Targets larger than 2 m in diameter will not lead to significant improvements. In addition, a two-concentric-circle design (the inner circle has one-half the radius of the outer circle) with different coatings can produce considerable accuracy improvements in the horizontal position. Details and performance evaluation can be found in (Csanyi and Toth, 2007).

3. LIDAR INTENSITY DATA

The introduction of intensity data a few years ago produced unrealistically high initial expectations. On one side, the visualization value provided a major help for interactive processing, and thus, users could immediately benefit from the new source of data, as LiDAR intensity was comparable to optical image type of data that had been missed by practitioners from the early beginning. On the other side, the algorithmic advantages of using intensity data for providing better LiDAR data processing were largely overestimated. While research instantly started to address the exploitation of the new source of information, the problem seemed to be harder than expected. In simple terms, the major difficulty of working with LiDAR intensity data is the relative nature of this signal. For example, different surfaces, data from different flying heights, and different surface orientations can produce exactly the same intensity values. Therefore, techniques to calibrate the intensity and range values with respect to each other started to become more common.

One of the first attempts on using intensity data dates back to the time when LiDAR intensity data were not yet commercially available. Maas (2001) describes the extension of a TIN-based matching technique using reflectance data (LiDAR intensity data) to replace surface height texture for the determination of planimetric strip offsets in flat areas with sufficient reflectance texture. As an extension, Vosselman (2002) offers another solution, kind of a feature-based matching, to avoid interpolation of the data, using linear features, gable roofs, and ditches, modeled by analytical functions that can provide accurate offset determination. Later, research interest steered toward conventional classification use of the intensity data. Song et al. (2002) proposed a technique to use intensity data for land-cover classification. A similar study on using intensity for glacier classification is presented in Lutz et al. (2003). A recent review of more advanced versions of these techniques is offered by Hasegawa (2006). A comprehensive study on processing both range and intensity data is provided by Sithole (2005). Kaasasalainen et al. (2005) provides a review on intensity data with respect to calibration. Nobrega and O'Hara (2006) compare two techniques for filtering intensity data for object extraction. Finally, Ahokas et al. (2006) presents the results of a calibration test on intensity data using the Optech ALTM 3100.

Figures 1 and 2 show simultaneously acquired orthoimage and the LiDAR intensity image, respectively, of an intersection. The LiDAR point density was about 4 pts/m^2 with foot print size of 15 cm. Note that the pavement markings in the LiDAR image are quite visible and distinct from the pavement. Consequently, if the approximate location of the pavement markings is known, then their extraction is a fairly straightforward task.

To illustrate that LiDAR elevation and intensity data are correlated and intensity information can indicate the presence of ranging error, Figure 3 shows the elevation data of the same intersection. Note that the pavement markings can be seen quite well, which conflicts with the fact that elevation value of the markings and the pavement around them should be identical (the few mm thickness of the markings is negligible compared to the few cm ranging accuracy of the laser system). This phenomenon is known and correction tables are available to partially compensate for this effect. The importance of this anomaly from our perspective is that during the comparative analysis later, the elevation value of the markings should be replaced by the average elevation of the pavement.

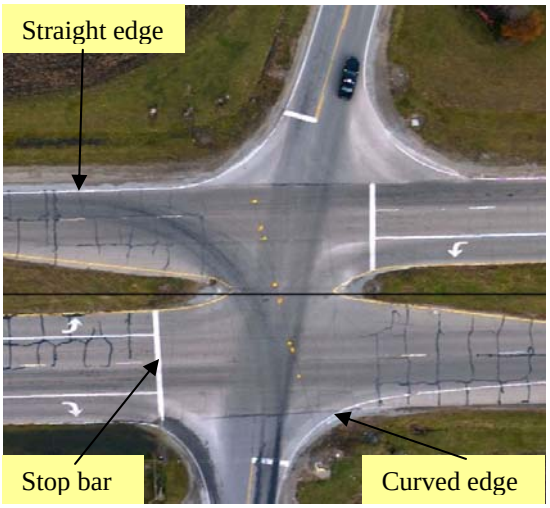

Figure 1. Typical pavement markings at an intersection.

Figure 2. LiDAR intensity image.

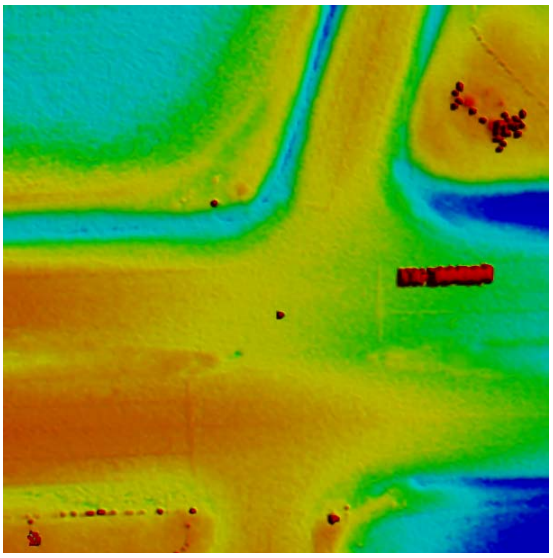

Figure 3. LiDAR elevation data.

4. EXTRACTING PAVEMENT MARKINGS AND USING THEM AS GROUND CONTROL

The concept of the proposed method, including pavement marking extraction as well as parameterization of the marks based on LiDAR intensity data, the comparison with ground truth, and the determination of a transformation to correct the point cloud, analysis of result, etc., is shown in Figure 4. General assumptions are that the survey data of the pavement markings are available a priori and the individual point accuracy, describing the marks, is known at the cm-level. To achieve good performance, sufficient number of pavement markings is required with good spatial distribution. At this point only three types of pavement markings are considered: Stop bars, straight edge lines and curved edge lines; Figure 1 shows the three pavement marking types. The survey data of the pavement markings is provided as point observations along the centerline of the markings. The LiDAR data, including range and intensity components, are assumed to be of reasonable quality; i.e., the point cloud accuracy is better than a meter.

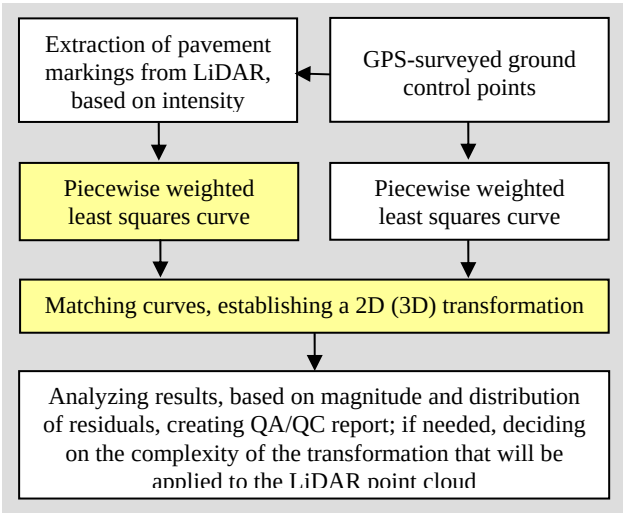

Figure 4. Block diagram of the proposed method.

Based on the comparison of the two descriptions of pavement markings, one obtained from the GPS survey and the other one form LiDAR intensity data, offset and orientation differences can be detected. Depending on the magnitude of the observed differences and their spatial distribution, a variety of corrections can be applied to the LiDAR point cloud to improve the point position accuracy. For example, if there is a similar vertical shift detected at the control features, a common vertical offset correction can be applied. If the amount of vertical shift detected varies by location and/or combined with non negligible horizontal differences, a more complex model, such as a 3D similarity transformation can be applied. Note that assessing the horizontal accuracy is difficult, as it is mainly defined by the footprint of the laser pulse, which depends on flying height and beam convergence; in addition, the impact of object surface characteristics could be also significant. The transformation based on the observed differences can be formulated on both, point- and linear feature-based least squares adjustment techniques. The conventional control point-based method is rather straightforward; similar to an absolute orientation of a stereo model with fixed scale. Linear feature-based orientation is less widely used, but could be feasible given the availability of matched linear features. Finally, if the differences are out of

the usual range (gross errors), the process can indicate system malfunctioning.

In our case, the point-based transformation is directly not applicable, as there is no point-to-point correspondence between the two point sets that describe the same linear feature. Assuming that the two representations provide an adequate description of the same shape, the problem is simply how to match two free-shape curves. In the following, the two key components of the proposed method, curve fitting and matching are discussed at detail.

4.1 Curve fitting

The extracted LiDAR points of the pavement markings and their surveyed data should be modeled as linear features in order to be matched with each other. The selected method is an extended version of the algorithm, originally proposed by Ichida and Kiyono in 1977, and is a piecewise weighted least squares curve fitting based on cubic (third-order polynomial) model, which seemed to be adequate for our conditions. To handle any kind of curves, defined as the locus of points f(x, y) = 0 where f(x, y) is a polynomial, the curve fitting is performed for smaller segments in local coordinate systems, which are defined by the end points of the curve segments. The primary advantage of using a local coordinate system is to avoid problems when curves become vertical in the mapping coordinate system. Figure 5 shows the concept of the local coordinate system used for curve fitting; obviously, the fitting results as well as the fitting constraints are always converted forth and back between the local and mapping coordinate frames.

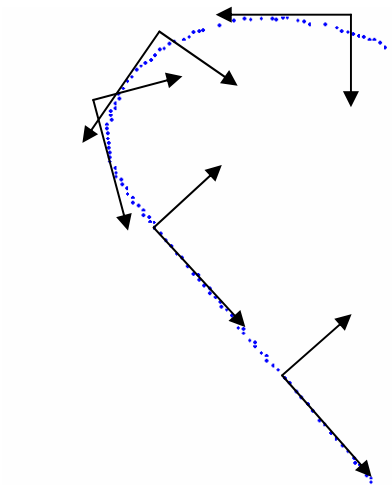

Figure 5. The curve fitting is done in local coordinate system, oriented to curve segment.

The main steps of the piecewise cubic fitting (PCF) process are shortly discussed below; the notation used in the discussion is introduced in Figure 6. To achieve a smooth curve, the curve fitting to any segment is constrained by its neighbors by enforcing an identical curvature at the segment connection points; in other words, PCF polynomial is continuous with its first derivative at connection points *x=s, x=t*, etc. The equations describing the third-order polynomial and its first derivative are:

$$S_k(x) = y_s + m_s \cdot (x-s) + a_s \cdot (x-s)^2 + b_s \cdot (x-s)^3$$

$$\text{slope} = S_k'(x) = m_s + 2 \cdot a_s \cdot (x-s) + 3 \cdot b_s \cdot (x-s)^2$$

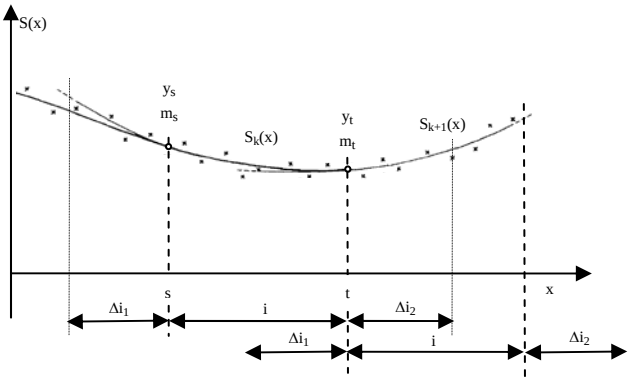

Figure 6. Piecewise weighted least squares curve fitting method.

The core processing includes the following steps: 1) a_S and b_S, the coefficients of the second and third order terms of the fitted curve for interval '*i*' are estimated; consider the constant term (y_S) and the coefficient of the first order term (m_S) fixed, known from the curve fitting from the previous segment. In the adjustment, the points in interval $\Delta i_2 + i + \Delta i_1$ (past, present, and future data points) are used, 2) the value (y_t) and the slope (m_t) at $x=t$ are computed; these values as fixed constraints are used in the curve fitting for the next segment, and 3) step 1 is repeated to process the next segment.

Step 1	$y - y_s - m_s \cdot (x-s) = a_s \cdot (x-s)^2 + b_s \cdot (x-s)^3$ LS for points in interval $\Delta i_1 + i + \Delta i_2 \Rightarrow \hat{a}_s, \hat{b}_s$ $\Rightarrow S_k(x) = y_s + m_s \cdot (x-s) + \hat{a}_s \cdot (x-s)^2 + \hat{b}_s \cdot (x-s)^3$
Step 2	$\rightarrow x = t$ $\hat{y}_t = S_k(t) = y_s + m_s \cdot (t-s) + \hat{a}_s \cdot (t-s)^2 + \hat{b}_s \cdot (t-s)^3$ $\hat{m}_t = S_k'(t) = m_s + 2 \cdot \hat{a}_s \cdot (x-s) + 3 \cdot \hat{b}_s \cdot (x-s)^2$ $\rightarrow y_t = \hat{y}_t \;\; and \;\; m_t = \hat{m}_t$
Step 3	$S_{k+1}(x) - y_t - m_t \cdot (x-t) = a_t \cdot (x-t)^2 + b_t \cdot (x-t)^3$ LS for points in interval $\Delta i_1 + i + \Delta i_2 \Rightarrow \hat{a}_t, \hat{b}_t$

4.2 Matching curves

Iterative registration algorithms are increasingly used for registering 2D/3D curves and range images recently. The well-known Iterative Closest Point (ICP) algorithm (Besl and McKay, 1992; Madhavan et al., 2005) is adopted here to match curves describing pavement markings obtained from LiDAR intensity and GPS measurements. The ICP algorithm finds the best correspondence between two curves (point sets) by iteratively determining the translations and rotations parameters of a 2D/3D rigid body transformation.

$$\min_{(R,T)} \sum_i \left\| M_i - (RD_i + T) \right\|^2$$

Where R is a 2*2 rotation matrix, T is a 2*1 translation vector and subscript i refer to the corresponding points of the sets M (model) and D (data). The ICP algorithm can be summarized as follows:

1. For each point in D, compute the closest point in M
2. Compute the incremental transformation (R, T)
3. Apply incremental transformation from step (2) to D
4. If relative changes in R and T are less than a given threshold, terminate, otherwise go to step (1)

Our 2D ICP was implemented in Matlab and space-scale optimization was incorporated to reduce execution time.

5. EXPRIMENTAL RESULTS

To perform an initial performance test of the proposed method, a typical intersection was selected from a recently flown LiDAR survey, where GPS-surveyed pavement markings were available. Figure 7 shows the area with linear pavement markings measured from the LiDAR intensity data as well as the GPS points. Note the clearly visible misfit between the two point sets; the horizontal accuracy of the GPS-surveyed points, provided by the Ohio Department of Transportation VRS system is 1-2 cm.

The LiDAR point-based description of the pavement markings was obtained by filtering. The search space was defined by the GPS control points (pavement markings are assumed to be within ±1 m of their true location) and intensity thresholding was used to extract the linear features; the road pavement has low intensity value while the pavement markings exhibit higher intensities. The threshold is adaptively defined by analyzing the histogram of the LiDAR intensity values of the road surface around the surveyed road pavement markings and/or by examining intensity values of road surface profiles (LiDAR scan-lines).

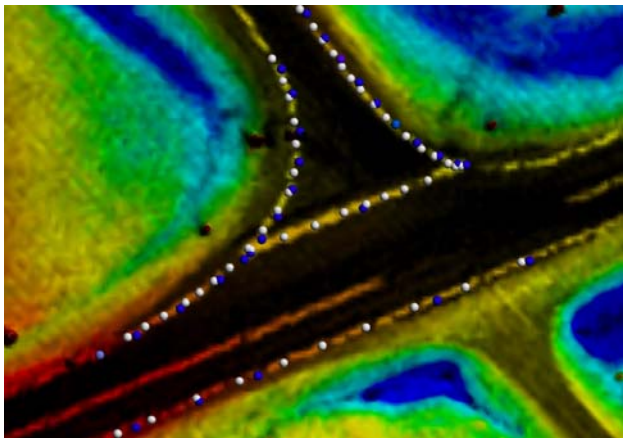

Figure 7. Intersection with pavements markings measured from LiDAR intensity data (white) and GPS-surveyed (blue).

In the curve-fitting step, both representations of the linear features are computed according the algorithm described in 4.1. Figure 8 shows one example of the fitted curves for the west curb line.

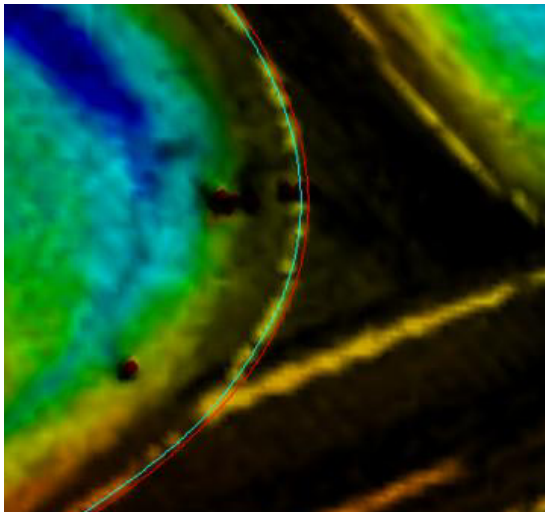

Figure 8. Curve fitting based on LiDAR and GPS points.

The results of the ICP-based curve matching for all the four curve lines is shown in Figure 9. Visually, the transformation shows a good fit; the blue points nicely fall on the GPS-defined curves. Note that the original curve points, derived from LiDAR, moved to the control curve similarly, as opposed to they would move if the individual curves had matched. Figure 10 shows the results of curve matching for the lower straight pavement line, including both the transformation results; as expected the individual transformation implements a perpendicular projection to the control curve.

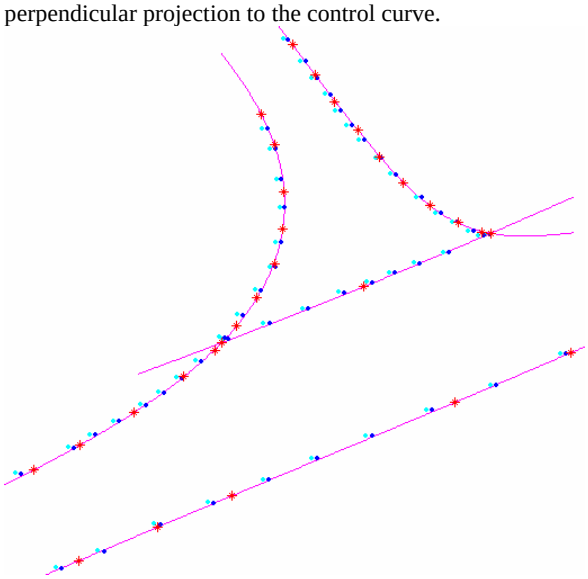

Figure 9. Curve matching based on all the four curves; magenta: curves fitted to control points, red: GPS control points, blue: curve points derived from LiDAR, and cyan: transformed curve points (derived from LiDAR).

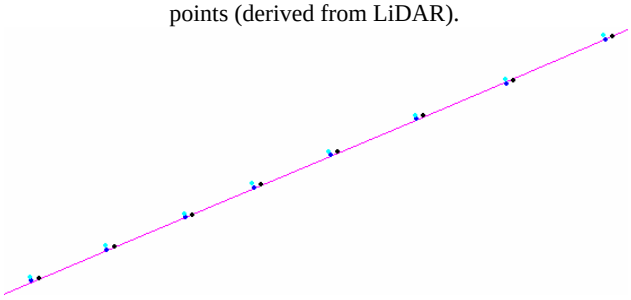

Figure 10. Comparing individual and combined curve fitting to a straight feature; magenta: reference curve, cyan: points derived from LiDAR, blue: transformed points based on single curve matching, and black: transformed points based on matching all the four curves together.

To assess in actual numbers the accuracy of the transformation, obtained by the ICP-based curve matching, correspondence between the LiDAR-derived curve and the control curve were established. Since the two curves in general are not totally identical, even after the final ICP iteration, the transformed LiDAR-derived points are close but not necessarily fall on the control curve. However, the location of the transformed LiDAR-derived points represents the best fit to the control curve in least squares sense. Therefore, these points are projected to the closest points of the control curve, and then they are considered as conjugate points. The transformation parameters between these two point sets (the original LiDAR-derived points and their corresponding points on the control curve) are calculated in a least squares adjustment. In this computation, the transformation parameters for the test data were estimated at $\sigma_{\Delta X} = \pm 0.013$m, $\sigma_{\Delta Y} = \pm 0.017$m, and $\sigma_{angle} = \pm 1.95$ arcmin, indicating that a good match was found with the

ICP method for the spatially well distributed test data set. The numerical values, including the transformation parameters, error terms, and dispersion matrix are listed in Tables I and II.

Transformation parameter	ICP-adjusted results [m, °]	Estimated accuracy [cm, °]
ΔX	0.46	0.013
ΔY	-0.08	0.017
φ	-0.09	0.03

Table I. Transformation results (2D).

1.0e-003 *	0.1789	-0.1699	-0.0063
	-0.1699	0.2902	0.0087
	-0.0063	0.0087	0.0003

Table II. A posteriori dispersion matrix.

The ~2 cm horizontal accuracy is reasonable given the fact that the GPS-surveyed points are known at 1 cm-level accuracy and the LiDAR-based pavement marking positioning accuracy is estimated at the few cm range.

6. CONCLUSION

The introduced method to automate the use of pavement markings as ground control showed good initial performance. Both the curve fitting and ICP-based matching delivered robust results. Further research will consider the extension of technique to 3D.

References:

Ahokas, E., Kaassalainen, S., Hyyppa, J. and Suomalainen, J., 2006. Calibration of the Optech ALTM 3100 Laser Scanner Intensity Data Using Brightness Targets, Proceedings of ISPRS Commission I. Symposium.

ASPRS LiDAR Committee, 2004. ASPRS Guidelines Vertical Accuracy Reporting for LiDAR Data

http://www.asprs.org/society/committees/lidar/Downloads/Vertical_Accuracy_Reporting_for_Lidar_Data.pdf

Baltsavias, E.P., 1999. Airborne Laser Scanning: Basic Relations and Formulas. ISPRS Journal of Photogrammetry & Remote Sensing, Vol. 54: 199-214.

Besl, P. J. and McKay, N. D. A method for registration of 3-d shapes. IEEE Trans. Pat. Anal. and Mach. Intel. 14(2), pp 239-256, Feb 1992.

Burman, H. ,2002. Laser Strip Adjustment for Data Calibration and Verification. International Archives of Photogrammetry and Remote Sensing, 34 (Part 3A): 67-72.

Crombaghs, M. J.E., R. Brügelmann, E.J. de Min, 2000. On the Adjustment of Overlapping Strips of Laseraltimeter Height Data. International Archives of Photogrammetry and Remote Sensing, 33, (Part B3/1):224-231.

Csanyi N, Toth C., Grejner-Brzezinska D. and Ray J., 2005. Improving LiDAR data accuracy using LiDAR-specific ground targets, ASPRS Annual Conference, Baltimore, MD, March 7-11, CD-ROM.

Csanyi, N. and Toth, C., 2007. Improvement of LiDAR Data Accuracy Using LiDAR-Specific Ground Targets, Photogrammetric Engineering & Remote Sensing, Vol. 73, No. 4, pp. 385-396.

Filin, S., and Vosselman, G., 2004. Adjustment of Airborne Laser Altimetry Strips. International Archives of Photogrammetry, Remote Sensing and Spatial Information Sciences 34 (Part B) pp. 285-289.

Hasegawa, H., 2006. Evaluations of LiDAR Reflectance Amplitude Sensitivity Towards Land Cover Conditions, Bulletin of the Geographical Survey Institute, Vol. 53.

Ichida, K. and Kiyono, T.1977. Curve Fitting with One-Pass Method with a Piecewise Cubic Polynomial, ACM Transactions on Mathematical Software, Vol. 3, No. 2, pp. 164-174.

Kager, H. and Kraus, K., 2001. Height Discrepancies between Overlapping Laser Scanner Strips. Proceedings of Optical 3D Measurement Techniques V, Vienna, Austria: 103-110.

Kaassalainen, S., Ahokas, E., Hyyppa, J. and Suomalainen, J., 2005. Study of Surface Brightness from Backscattered Laser Intensity: Calibration of Laser Data, IEEE Geoscience and Remote Sensing Letters, 2(3):255-259.

Kilian J., Haala, N., Englich, M., 1996. Capture and Evaluation of Airborne Laser Scanner Data. International Archives of Photogrammetry and Remote Sensing, 31 (Part B3):383-388.

Leica Geosystems, ALS50, http://gis.leica-geosystems.com

Lutz, E., Geist, Th. and Stötter, J., 2003. Investigations of Airborne Laser Scanning Signal Intensity on Glacial Surfaces - Utilizing Comprehensive Laser Geometry Modeling and Orthophoto Surface Modeling (A Case Study: Svartisheibreen, Norway), proceedings of ISPRS Commission III, WG 3.

Maas, H.-G., 2001. On the Use of Pulse Reflectance Data for Laserscanner Strip Adjustment. International Archives of Photogrammetry, Remote Sensing and Spatial Information Sciences, 33 (Part 3/W4): 53-56.

Madhavan, R., Hong, T., Messina, E. Temporal Range Registration for Unmanned Ground and Aerial Vehicles, Journal of Intelligent and Robotic Systems, Volume 44, Number 1 / September, 2005, pp. 47-69.

Nobrega, R. and O'Hara, C., 2006. Segmentation and Object Extraction from Anisotropic Diffusion Filtered LiDAR Intensity Data.

Optech, ALTM 3100AE, 2006, www.optech.ca/pdf/Brochures/ALTM3100EAwspecsfnl.pdf

Schenk, T., 2001. Modeling and Analyzing Systematic Errors in Airborne Laser Scanners. Technical Notes in Photogrammetry, vol. 19. The Ohio State University, Columbus, USA.

Sithole, G., 2005. Segmentation and Classification of Airborne Laser Scanner Data, Publication of Geodesy 59, Nederlandse Commissie voor Geodesie, Delft (184 pages).

Song, J-H., Han, S-H., Yu, K, and Kim, Y., 2002. Assessing the Possibility of Land-Cover Classification Using LiDAR Intensity Data, International Archives of Photogrammetry, 34. pp. 4.

Toth C., Csanyi N. and Grejner-Brzezinska D. 2002. Automating the Calibration of Airborne Multisensor Imaging Systems, Proc. ACSM-ASPRS Annual Conference, Washington, DC, April 19-26, CD ROM.

Toth, C. and Grejner-Brzezinska, D., 2005. Geo-referenced Digital Data Acquisition and Processing Systems Using LiDAR Technology – Final report, ODOT State Job No. 147990.

Vosselman, G., and Mass, H.-G., 2001. Adjustment and Filtering of Raw Laser Altimetry Data. Proc. OEEPE Workshop on Airborne Laserscanning and Interferometric SAR for Detailed Digital Elevation Models. OEEPE Publication 40, Stockholm, Sweden. pp. 62-72.

Vosselman, G., 2002. On the Estimation of Planimetric Offsets in Laser Altimetry Data. International Archives of Photogrammetry and Remote Sensing, 34 (Part 3A): 375-380.

Vosselman, G., 2002. Strip Offset Estimation Using Linear Features. 3rd International LIDAR Workshop, October 7-9, Columbus, http://www.itc.nl/personal/vosselman/papers/vosselman2002.columbus.pdf